Mine Water and the Environment (2019) 38:556–565
https://doi.org/10.1007/s10230-019-00612-6

TECHNICAL COMMUNICATION

Hydrochemical Evolution of the filling of the Mining Lake of As Pontes (Spain)

Ricardo Juncosa[1] · **Jorge Delgado**[1] · **Jose Luis Cereijo**[1] · **Andrea Muñoz**[1]

Received: 6 February 2019 / Accepted: 15 May 2019 / Published online: 29 May 2019

Abstract

The old As Pontes lignite mine is located in northwest Spain, in the Galicia region. Filling of the 547 hm^3 pit began at the end of January 2008 through the controlled input of surface water. The filling was completed on April 18, 2012, leading to a steady water regime. During this process, both the water input and the water stored in the pit were hydrochemically monitored. The water chemistry in the superficial area of the lake, as well as the chemical stratification, are presented.

Keywords Mining restoration · Chemocline · Water quality · Hydrology

Introduction

The As Pontes de García Rodríguez mine pit is located in the Galicia region and northwest Spain in the Eume River basin (Fig. 1). The mine is located in a lignite deposit in the Tertiary sedimentary basin, which has a tectonic origin. The substrate of the deposit is composed of phyllites, schists, quartzites, greywacke, meta-arkoses, and gneisses and was affected by the Hercynian orogeny. The deposit features clays and sand alternating with lignite (Juncosa et al. 2018).

Once mining ceased at the end of 2008, the pit began to be filled with water diverted from the Eume River and nearby basins (Juncosa et al. 2018). These basins have a catchment area of approximately 207 km^2. The mean annual rainfall of the area is ≈ 2000 mm. The As Pontes mine pit has been filled for 4.5 years. The current lake has an area of ≈ 8.1 km^2, and is 5 km in length with a NW–SE orientation, and has a maximum width of 2.2 km. The pit is full to levels 127 to 332 m above sea level, with a maximum depth of 205 m (Juncosa et al. 2018).

The chemical quality of the lake has depended on many factors, including the type of material exploited (lignite), the type of embedding rock (mainly phyllite) (Hirji and Davis 2009), the climate, the filling time (Juncosa et al. 2016), and the morphometry of the pit (Boland and Padovan 2002; Castro and Moore 2000; Werner et al. 2001a, b).

The lake received water from various points in the North, South, East and West Channels. The East Channel provided the greatest volumetric contribution to the lake since it received water diverted from the Eume River as well as other minor inputs. Other contributions, less significant in volume but relevant in terms of the chemical quality, came from flows originating in the external dump, the runoff from the walls of the slopes into the pit, and groundwater (Castendyk and Eary 2009; Castendynk and Webster-Brown 2007a, b; Denimal et al. 2005; Padilla et al. 2015; Schultze et al. 2010; Younger and Wolkersdorfer 2004). In this article, we investigated the chemical and physical processes that likely occurred during the filling of the mine pit.

Materials and Methods

The morphology of the lake changed during progressive flooding of the pit, and several water bodies appeared and disappeared: Campo Este (PVE), Umbral (LU), and Campo Oeste (PVO) (García-Rádade et al. 2014; Hernández et al. 2012). Umbral disappeared as an independent water body in April 2008, so throughout 2009, the distinction between the Camp Este (PVE) and Umbral (LU) samples only reflects the original location of the latter. At the end of 2009, these water bodies merged into a single body (Fig. 2) whose bathymetry evolved with the flooding. The monitoring of the lake filling process was carried out at three different points, representing

---

✉ Ricardo Juncosa
rjuncosa@udc.es

[1] School of Civil Engineering, University of A Coruña, Campus de Elviña s/n., 15192 A Coruña, Spain

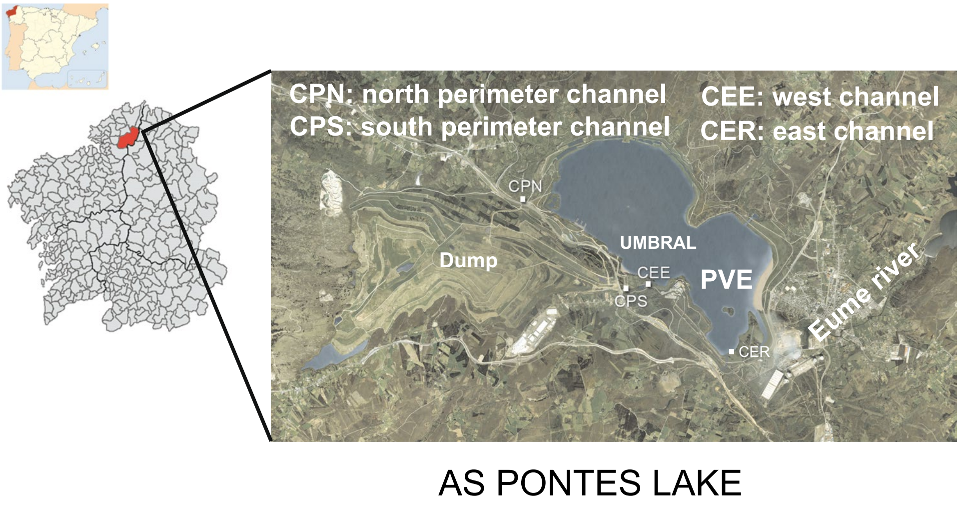

Fig. 1 Location of the As Pontes lake

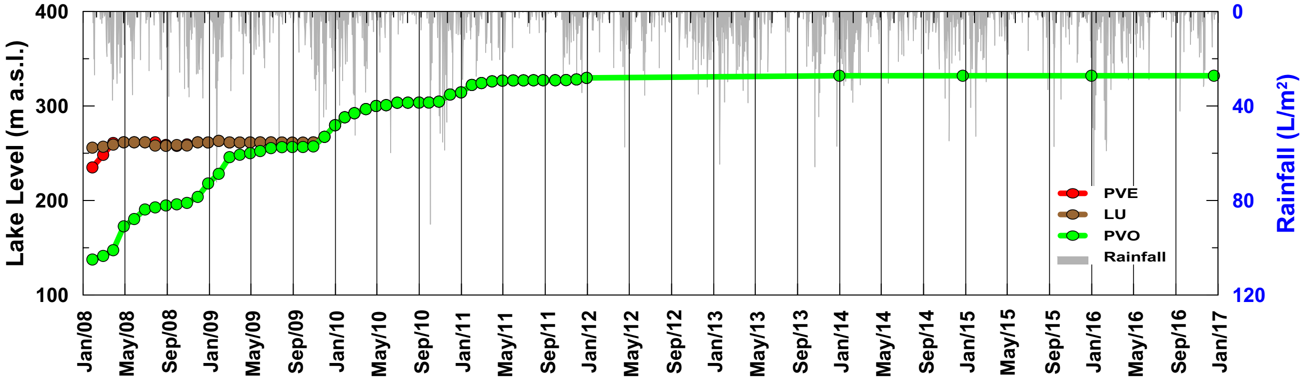

Fig. 2 Temporal evolution of water level (masl)

the three initial water bodies. Figure 2 shows the water level and precipitation data.

The water sampling and the applied analytical procedures were carried out according to APHA (1998). The temperature, specific conductivity, pH, dissolved oxygen concentration, and oxidation/reduction potential were always determined at the same sampling points (Juncosa et al. 2018). The sulphate concentrations were determined using an ionic chromatograph 850 Professional IC (Metrohm).

Until August 2013, atomic adsorption spectroscopy was used to analyze the metals. After that, the analysis of cations and metals was carried out using a Thermo Finnigan ELEMENXR magnetic field inductively coupled plasma mass spectrometry (ICP-MS).

The depth sampling consisted of taking weekly samples from the surface (Delgado et al. 2013, 2014), every 5 m from the free layer (at 5, 10, 15, and 20 m), and every 10 m from that point on (30, 40, 50,…) during the filling process. The YSI 6600-V2 probe was used to obtain continuous vertical profiles of the physical parameters. Once the pit was filled, the sampling frequency was monthly.

The following parameters and concentrations were measured: pH, Al, As, Ba, B, Cd, Cr_{total}, Fe_{total}, Fe_{dis}, Mn, Ni, Hg, Pb, Se, Cu, Zn, Ti, Cl, F, SO_4, P_{total}, PO_4, N_{total}, NO_3, NO_2, NH_4, DBO_5, temperature, specific conductivity, oxidation/reduction potential, dissolved oxygen, alkalinity, Li, Na, K, Ca, Mg, SiO_2, Br, COD, CID, Ag, Co, Mo, Sb, U, V, S, bicarbonate and stable oxygen and hydrogen isotopes (Delgado et al. 2008a, b, 2010, 2011). These are all currently regulated by Spain and the European Community regulations (EC 2008, 2009; EPLWG 2004).

Results

Filling the Pit

The controlled flooding of the As Pontes open pit mine began at the end of January 2008 and was completed in April 2012. Currently, the lake only receives precipitation, groundwater discharges, and inputs from its natural watersheds, with particularly large contributions from the Illade and

Meidelo Rivers. During these years, ENDESA Generación SA added lime through one of the streams that discharged into the lake. Figure 3 shows the balance of the lime inputs to the lake during this period. The same figure shows these inputs have significantly decreased since April 2010, ending in June 2013. The accumulated lime mass added to the lake during that period was 9531 t.

Surface Water of the Lake

Figure 4 shows the thermal evolution of the water inputs, as well as the evolution of the surface waters corresponding to PVE, PVO, and LU during 2009–2016. Seasonal distribution is evident, with maximums in August/September and minimums in January/February.

The high pH values observed in the surface waters of the lake throughout 2009 and until mid-2010 in PVE (former Campo Este) and LU (former Umbral) reflect the alkaline additions coming from the West Channel (Fig. 5). Thereafter, as the calcium hydroxide input rate decreased (Fig. 3), the contrast observed in PVE and LU blurs until it disappears. The highest pH values are associated with the CEE waters (West Channel), as the lime inputs came from that area (Fig. 5).

Once all of the water bodies unified (at the end of 2009), the pH differences between the observation points began to blur. As of the end of 2010, the surface water of the lake was homogeneous, at least in pH, with a narrow value range comparable to the CPN, CPS, and CEE inputs. Since the beginning of 2011, the temporal evolution of the pH has shown a seasonal behaviour, with slightly higher values in the summer.

Figure 6 shows that the CPN, CEE, and CPS inputs have higher conductivities with values that fluctuate significantly with precipitation. The highest conductivity was observed in the dry periods and the lowest in the monsoon season. This trend, which has been repeated over these years, is attributed to washing of the easily soluble mineral phases (diverse hydroxysulphates, etc.) formed in the dump areas and exposed slopes during the dry periods. With the advent of the monsoon season, these substances rapidly dissolved, resulting in discharge peaks of low chemical quality (concentrated in summer rains and distributed/decreasing in winter/spring).

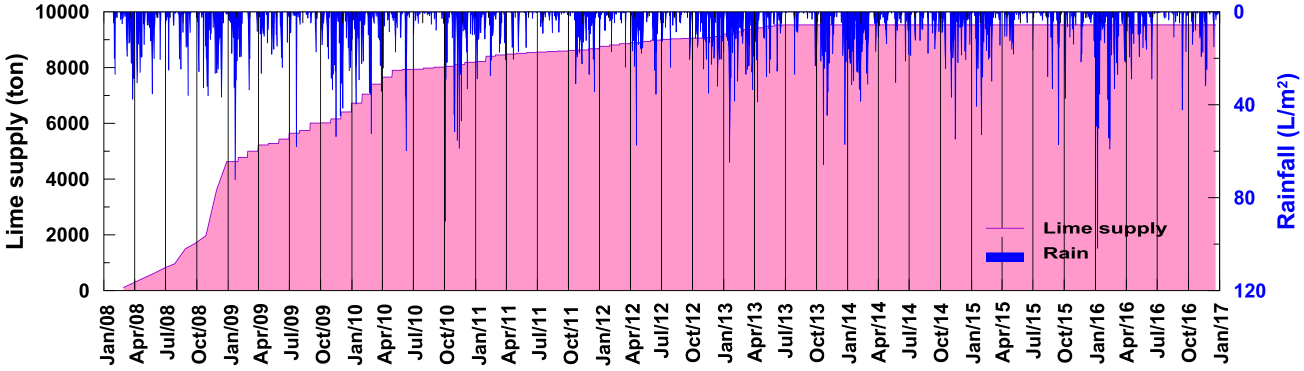

Fig. 3 Lime supply (accumulated mass of calcium hydroxide 2008–2016)

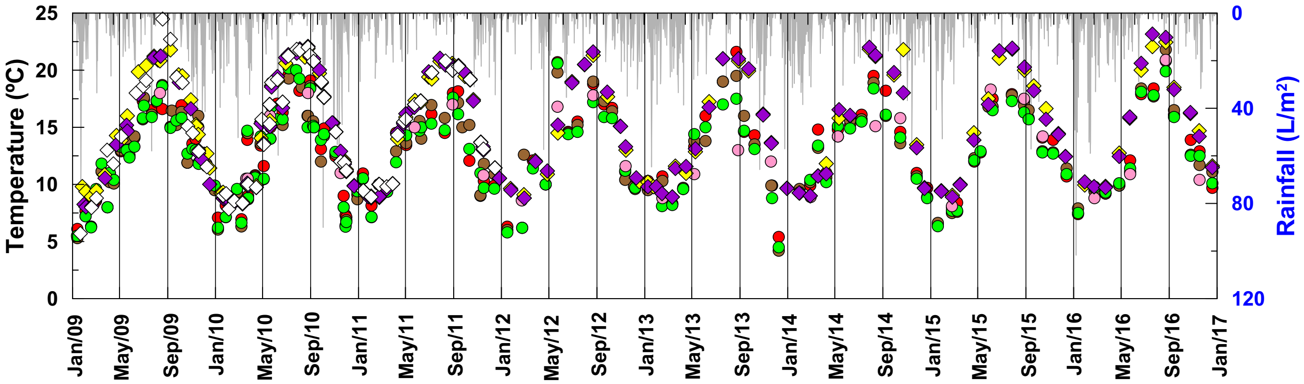

Fig. 4 Superficial waters: temporal evolution of temperatures in PVE, PVO, and LU lakes, and in the contributions of CPS, CPN, CEE, and the Eume River

Note that the conductivities observed in CPN and CPS do not correspond to those of the runoff/fluvial circulation typical of the area (which range between 50 and 250 µS/cm; the Eume River has values near the lower limit of this range). The observed (500 to 800 µS/cm) are consistent with a mix of rainwater and local streams with other inputs from the mine's external dump. In this sense, the restoration of the dump is the key to improving the quality of these waters by reducing the weathering (oxidation) of the collected materials.

Figure 7 shows the concentrations of dissolved oxygen in the surface waters of the lake. There is a pattern of thermal

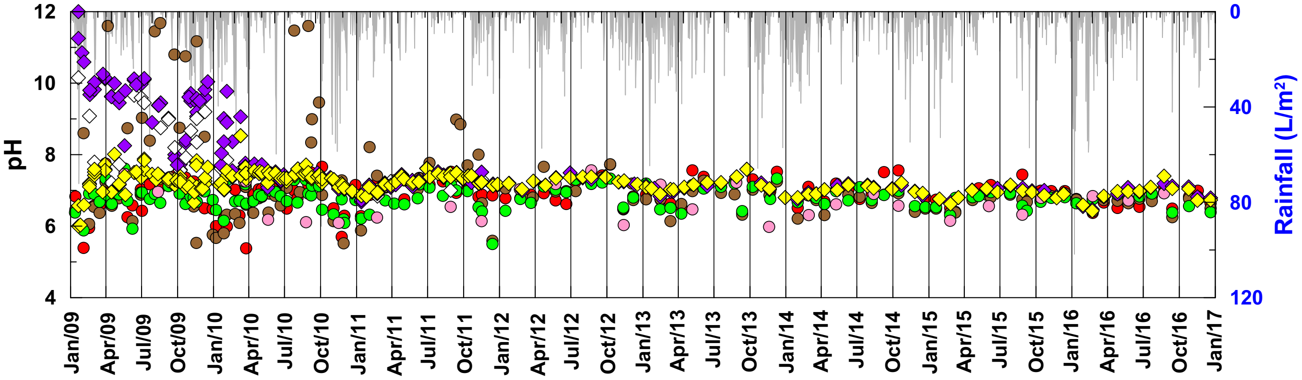

Fig. 5 Superficial waters: temporal evolution of pH in PVE, PVO, and LU lakes, and the contributions of CPS, CPN, CEE and the Eume River

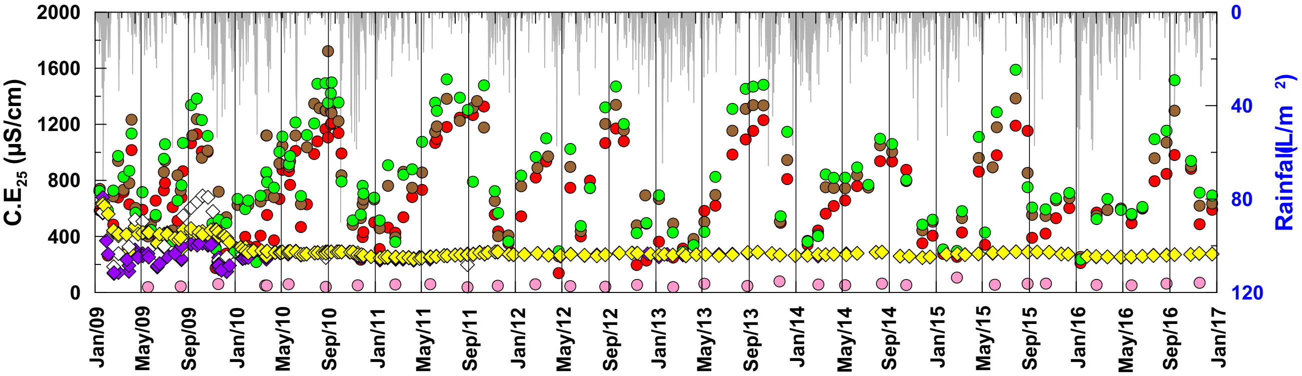

Fig. 6 Superficial waters: temporal evolution of conductivity in PVE, PVO and LU lakes, and in the CPS, CPN, CEE, and Eume River. The gray color strip shows the discharge limit for this parameter (500 µS/cm)

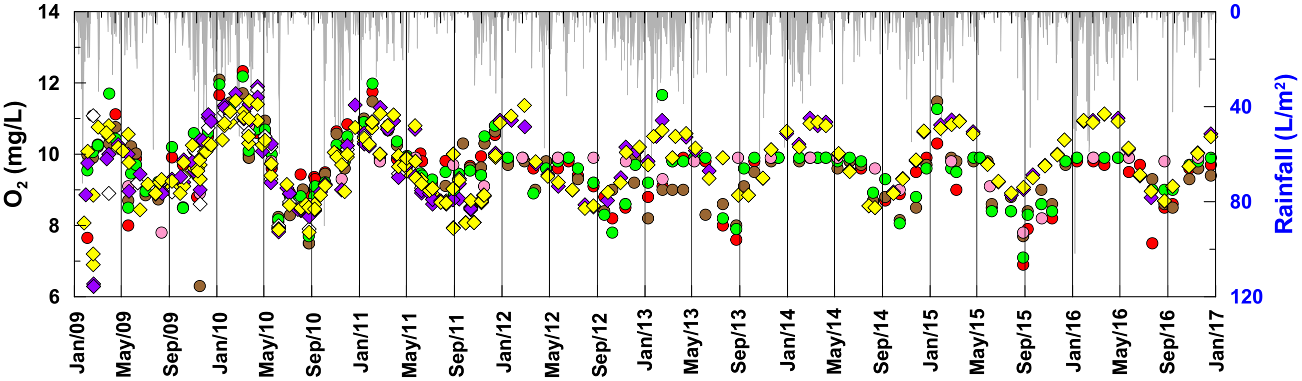

Fig. 7 Superficial waters: temporal evolution of dissolved oxygen in PVE, PVO, and LU lakes, and the contributions of CPS, CPN, CEE, and the Eume River

dependence due to climatic seasonality. Thus, the lowest O_2 concentrations occur in the summer (July/August), while the highest occur in the winter time (January/February).

The concentration of dissolved iron (Fig. 8) in the water shows a certain seasonal variability, and as with the conductivity, no significant changes were observed as time passes. However, a maximum threshold concentration (≈ 10 mg/L) was observed, above which Fe oxyhydroxide or hydroxysulfate precipitation occurred. Ferric iron (Fe^{+3}) and ferrous iron (Fe^{+2}) are potential sources of precipitates.

The concentration of iron is controlled mainly by the pH; at pH values above 7.2, the iron precipitates, decreasing dissolved iron concentrations to less than the atomic absorption detection limit (0.1 mg/L). So in August 2013, ICP-MS was used, establishing a new detection limit for dissolved iron of 1 µg/L (0.001 mg/L). This allowed a determination that the concentration of this element was very low (1.45 µg/L in August 2013), even less than that of the Eume River.

During 2015, the PVO sampling point recorded iron concentrations in the surface waters above this limit in all samplings. The PVE sampling point only recorded a measurable value once. The higher concentrations at the PVO point may be due to preferential flows from the dump. In 2016, a new detection limit for dissolved iron of 2 µg/L (0.002 mg/L) was established; all values were below this limit throughout 2016.

Figure 9 shows the temporal evolution of the dissolved Mn concentrations in the water inputs and the surface of the lake. The behaviours of CPN, CPS, and CEE were clearly seasonal, with maximum concentrations in the summers and minimum concentrations in the rainfall periods, as a consequence of mixing processes in perimeter streams with less concentrated natural waters.

As of February 2010, the Mn concentration was virtually identical over the entire surface of the lake, with a marked tendency to decrease when the rainfall was more intense (September–December 2010). In June 2011, a sharp drop in the Mn concentrations was observed, which may be due to the influence of pH on the mineral phases that regulate Mn concentrations. Since June 2011, the Mn concentrations in the lake surface have been stable, with

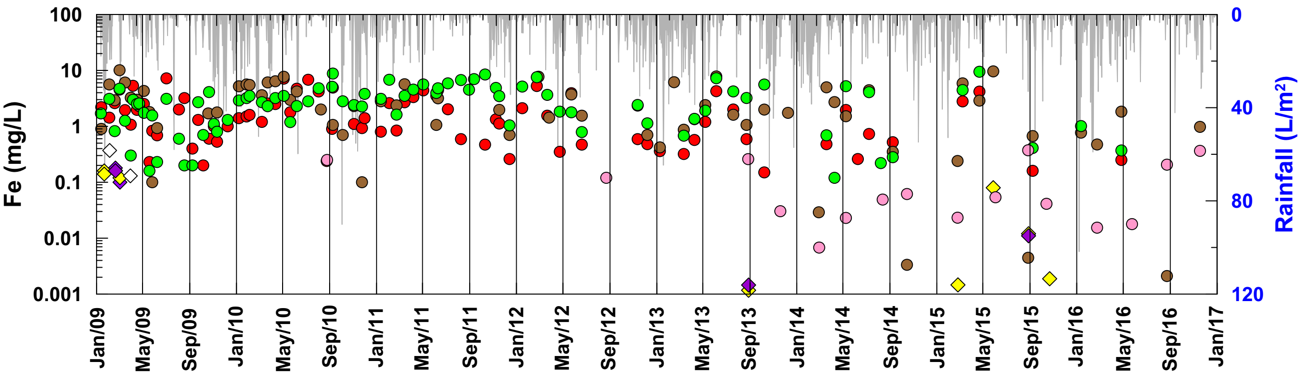

Fig. 8 Superficial waters: temporal evolution of disolved iron in PVE, PVO, and LU lakes, and the contributions of CPS, CPN, CEE and the Eume River. The gray color strip shows the discharge limit for this parameter (0.3 mg/L)

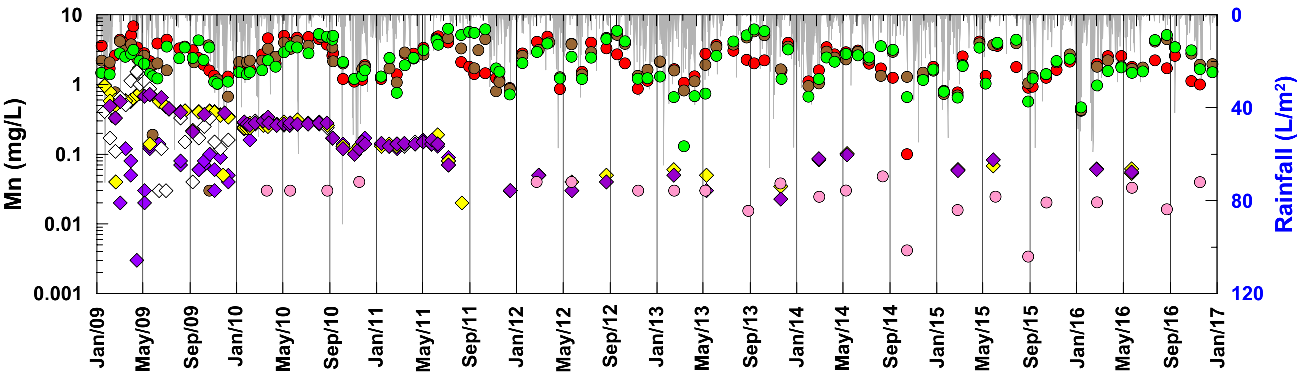

Fig. 9 Superficial waters: temporal evolution of disolved manganese in PVE, PVO, and LU lakes, and the contributions of CPS, CPN, CEE, and the Eume River. The gray color strip shows the discharge limit for this parameter (2 mg/L)

relatively constant values (≈ 0.04 mg/L), well below the legally prescribed limit of 2 mg/L).

Figure 10 shows the temporal evolution pattern of sulphate. The water from the external dump had the highest concentrations, which were greater in the dry periods than during heavy precipitation. These concentrations were well above the natural background and may reflect episodes of washing of the sulphate salts from the dump and their collection in an extensive channel and ditch network. Throughout 2015, the sulphate concentrations in the perimeter streams of the dump showed a less homogeneous behaviour than in previous years, possibly due to sampling at periods of low water flow that emphasized seasonal effects.

From the moment when water was no longer supplied from the Eume River, the sulphate concentrations in the surface waters of the lake experienced a slight upward trend. In this system (in which the solubility limits of relevant sulphate minerals cannot be reached), the concentration in the lake approximates the weighted average of the concentrations of each of the inputs (natural waters and rain, with concentrations of about 8 and 4 mg/L, respectively) that feed it.

Compound Evolution at Different Lake Levels

Figure 11 shows the thermal evolution at three points at different levels (the surface of the lake and at 250 and 160 m above sea level (masl), all of them located on the vertical line of the PVO point. It shows how the hypolimnion (level 250) remains isolated during a great part of the year but is thermally homogenized with the superficial layers during the first quarter of the year. It also shows that the temperature fluctuations during 2009 were similar to those of the surface. However, as of March 2010, when this point fell below the thermocline, it was exempt from the influence of the surface thermal oscillations, which did not prevent the surface temperatures at that level from equalling those of the first months of the year. The temperature at 160 masl (the deep

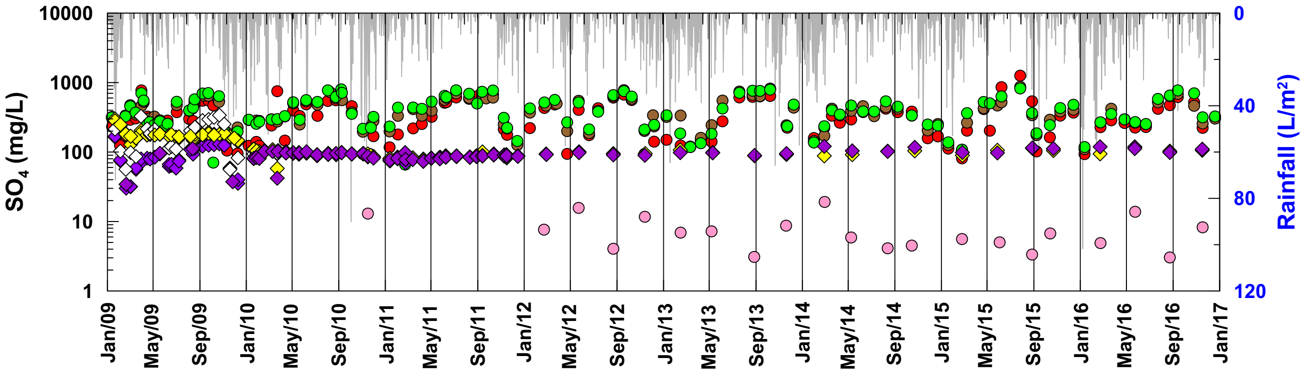

Fig. 10 Superficial waters: temporal evolution of disolved sulphate in PVE, PVO, and LU lakes, and the contributions of CPS, CPN, CEE, and the Eume River. The gray color strip shows the discharge limit for this parameter (250 mg/L)

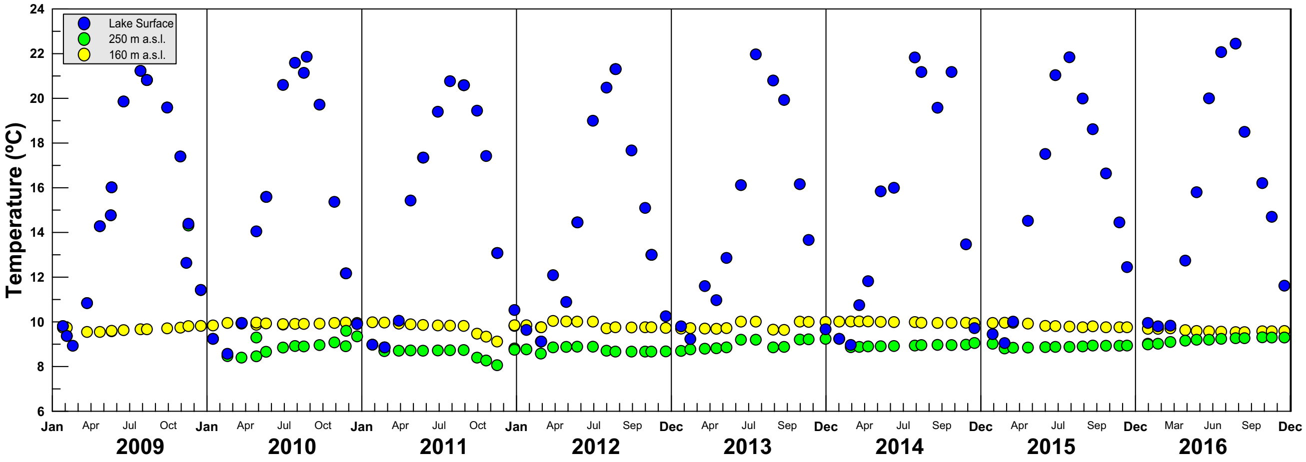

Fig. 11 Temporal evolution of temperature at the PVO point at levels 160, 250, and the surface. The flooding ended on April 18, 2012

zone of the lake) has remained virtually unchanged since the beginning of 2009, with a temperature almost equal to the temperature that existed during its isolation from the mixolimnion. The temporal evolution pattern at 160 and 250 masl, which remained constant until mid-2015, experienced a convergence towards the mean value recorded until then for those levels.

Since the end of 2010, the two water bodies (PVE and PVO) that make up the lake behaved homogeneously as the water bodies merged and the lime input decreased. The chemocline developed relatively quickly during December 2009, but did not stabilize until June 2010, because until then, its position was decreasing as the lake filled.

Likewise, acidification of the deep zone was very marked in 2009, with pH values greater than 6 in January/February and close to 4 when the chemocline was established in December. The pH stabilized there until the end of 2012, when an upward trend began. This increase could have been caused by the homogenization of the monimolimnion with the deepest waters (groundwater with higher pH) or by diffusive processes between the upper and lower layers to the chemocline. In this sense, the chemocline descent, ≈ 10 m at the beginning of 2014, could favour homogenization of the deepest zone.

The pH was practically constant throughout the water column (Fig. 12). The annual average pH of the surface water throughout 2016 (6.90) increased slightly, breaking the downward trend (7.37 in 2010, 7.3 in 2011, 7.3 in 2012, 7.12 in 2013, 7.00 in 2014, and 6.88 in 2015), although seasonal fluctuations were still more important within the same year.

Likewise, since 2014, a more abrupt pH decrease was observed in the hypolimnion, tending to converge towards a common value with the monimolimnion. Note that the water volume below the 200 level (43 hm^3 monimolimnion) is approximately 1/7th of the stored volume between levels 300 and 200 (287 hm^3 hypolimnion), so the resulting value will be very conditioned by the weighted mixture of these two volumes.

Figure 13 shows how the conductivity values in the deep zone (level 160), which remained constant since the occurrence of the chemocline (December 2009), has continuously declined since the beginning of 2012, reaching a value close to 380 µS/cm in December 2016. This decrease can be due to diffusion and mixing with the less concentrated upper layers of the lake or precipitation of dissolved solids (e.g. under anoxic conditions iron is reduced and precipitates as iron sulphide).

The conductivity data obtained from the water inputs (see Fig. 6) shows that both CPS and NPC have conductivity values (max 1000 µS/cm) that, combined with that of the main input from the Eume River (≈ 50 µS/cm), are compatible with the values of the superficial part of the lake. The new hydrographic configuration reached in April 2012 as a result of the overflow has not led to significantly different conductivities in the lake.

In turn, two clearly differentiated domains are identified: a superficial one in which the oxygenation moves up and down (due to mixing processes that occur to a depth of 110 m below the surface) and another involving a progressive decrease in the O_2 concentration (Fig. 14). The behaviour of the deep zone (level 160) throughout 2012, coinciding with the complete filling of the lake, breaks the trend of anoxic conditions present in previous years, maintaining O_2 concentration values constant at approximately 4 mg/L even in the deepest zone (the last 10 m), which, until 2012, was anoxic.

It is striking, however, how the O_2 concentrations have increased in depth since 2015. This increase implies a re-oxygenation, whose more plausible cause would be the mixing with shallower waters (Juncosa et al. 2018). This hypothesis is strengthened by noting the decrease in the oxygen

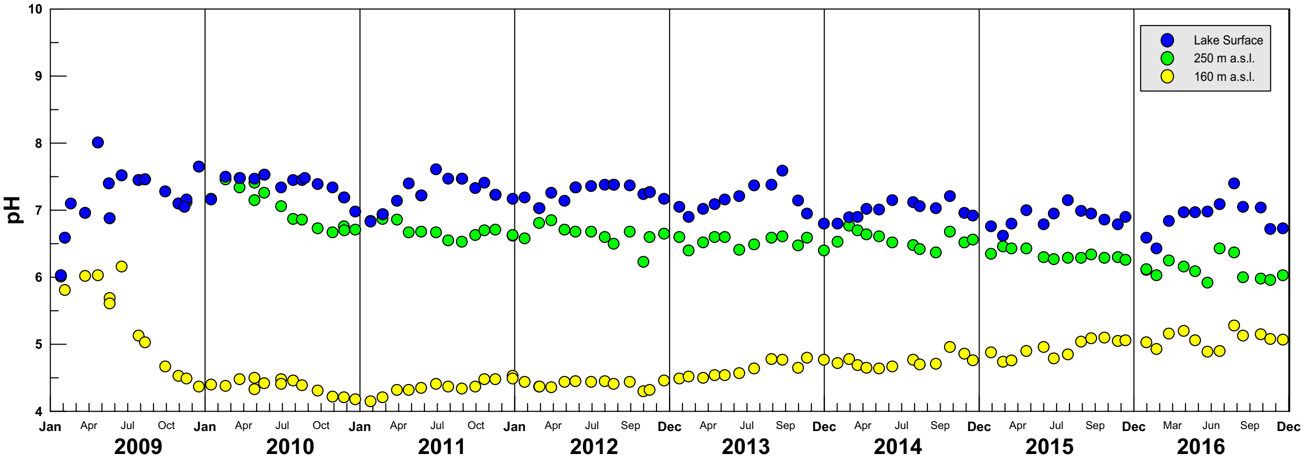

Fig. 12 Temporal evolution of pH at the PVO point at levels 160, 250, and at the surface. The flooding ended on April 18, 2012)

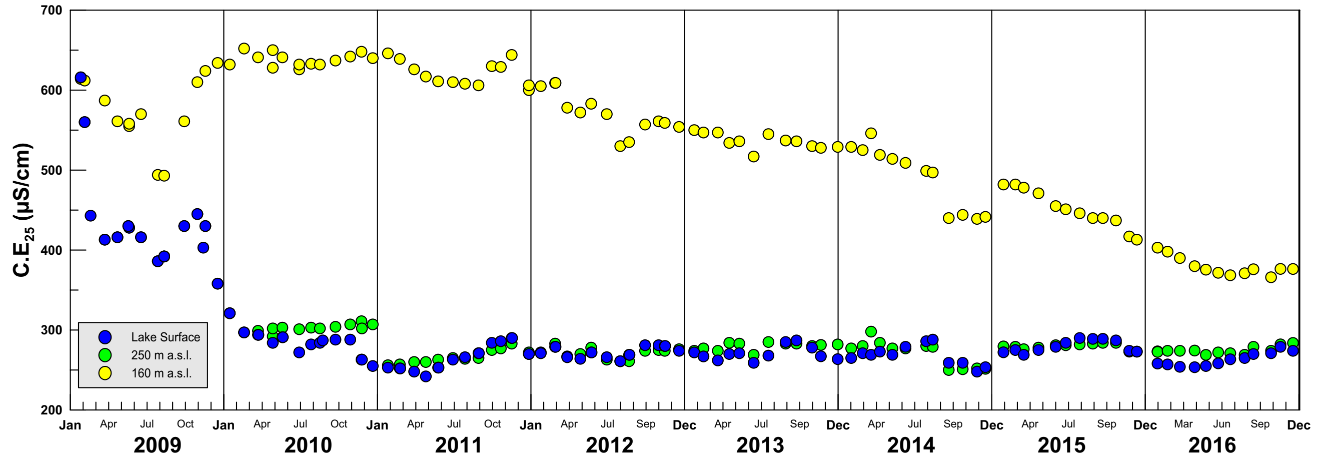

Fig. 13 Temporal evolution of conductivity at the PVO point at levels 160, 250, and at the surface. The flooding ended on April 18, 2012

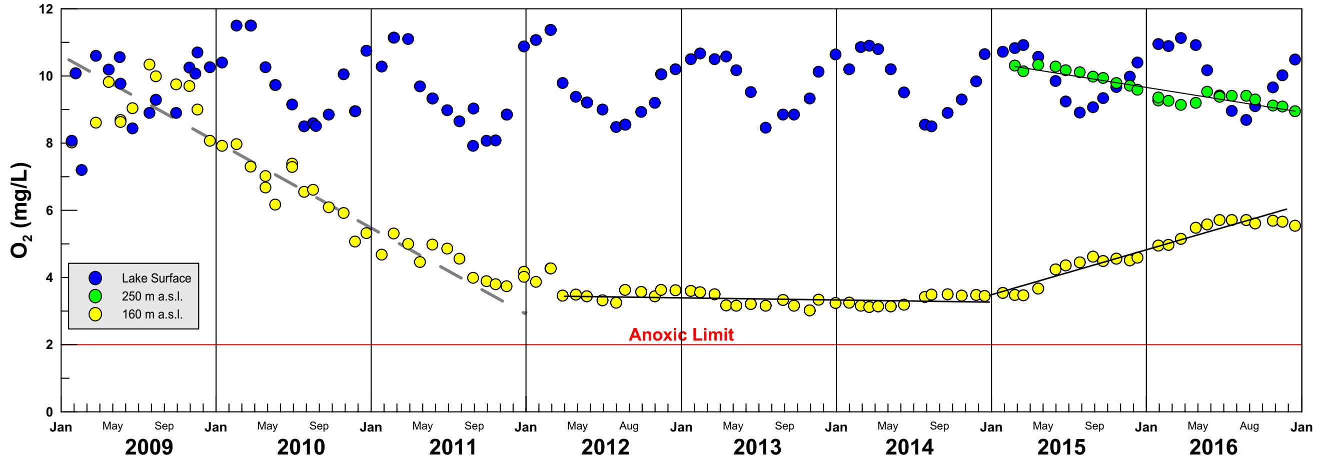

Fig. 14 Temporal evolution of disolved oxygen at the PVO point at levels 160, 250, and at the surface. The flooding ended on April 18, 2012

concentration at level 250. The difference between the oxygenation/deoxygenation slopes is explained by the difference in volumes involved in the mix. For example, in a totally closed system, a loss of 1 mg/L in a volume of 287 hm^3 would be equivalent to a gain of 6.7 mg/L in a volume of 43 hm^3. Regarding Fe, Mn, and sulphate, Juncosa et al. (2018) showed that their vertical profiles follow patterns dictated by pH and oxygen.

Conclusions

The old As Pontes mine pit was completely filled in April, 2012, which took 52 months and ≈ 548 hm^3 of water from runoff, the Eume River, direct precipitation, the external dump's diversion channels, and groundwater. The most important volumetric source was the Eume River. Partial diversion of water from the Eume River into the pit resulted in a better quality of lake water by reducing the potential oxidation of sulphides in the pit.

The lake continues to evolve and has not yet reached a steady state. The large volume of water stored in the pit gives it a very high chemical inertia, meaning that any physical–chemical change occurs at a very slow speed. In general, it seems that the chemocline located at level 220 tends to widen and its gradient tends to decrease as the system evolves, which means that the concentration differences between the hypolimnion and the monimolimnion are less pronounced each year.

Another noteworthy aspect is the evolution of the oxygen concentration on the bottom. After a few years of decrease (until 2012) and stabilization (until 2015), the oxygen concentration at depth has been increasing steadily. However, the concentration in the upper layer is gradually decreasing due to the oxygen transfer between the hypolimnion and the monimolimnion, although at a slower rate than the oxygenation.

The conductivity at the bottom has also tended to decrease gradually from 2012 due to homogenization with the upper layers. Thermal and chemical homogenization of the surface waters of the lake occurs due to thermal inversion at the beginning of winter (November/December). The thermal stratification in the summer is only 40 m below the surface, leaving the lower volume of water disconnected from the seasonal mixing.

Acknowledgements We want to give special thanks to ENDESA GENERACION. Funds for this work were provided by the Ministry of Science and Innovation (CGL2008-05940/BTE) and the European Regional Development Funds 2013/2017.

References

APHA (1998) Standard methods for the examination of water and wastewater. 20th edit, American Public Health Assoc, American Water Works Assoc, Water Environment Federation, Washington DC

Boland KT, Padovan AV (2002) Seasonal stratification and mixing in a recently flooded mining void in tropical Australia. Lakes Reserv Resour Manag 7:125–131. https://doi.org/10.1045/j.1440-169X.2002.00176.x

Castendyk DN, Eary LE (2009) The nature and global distribution of pit lakes. In: Castendyk DN, Eary LE (eds) Mine Pit Lakes: characteristics, predictive modeling and sustainability, management technolologies for metal mining influenced waters, vol 3. Soc for mining. Metallurgy and Exploration, Littleton, pp 1–8

Castendyk DN, Webster-Brown JG (2007a) Sensitivity analyses in pit lake prediction, martha mine, New Zealand 1: relationship between turnover and input water density. Chem Geol 244:42–55. https://doi.org/10.1016/j.chemgeo.2007.06.004

Castendyk DN, Webster-Brown JG (2007b) Sensitivity analyses in pit lake prediction, martha mine, New Zealand 1: geochemistry, water-rock reactions, and surface adsorption. Chem Geol 244:56–73. https://doi.org/10.1016/j.chemgeo.2007.06.005

Castro JM, Moore JN (2000) Pit lakes: their characteristics and the potential for their remedation. Environ Geol 39(11):1254–1260. https://doi.org/10.1007/s002549900100

Delgado J, Juncosa R, Vazquez A, Falcón I, Canal J, Hernández H, Padilla F, Vellando P, Delgado JL (2008a) Hydrochemical characteristics of the natural waters associated with the flooding of the Meirama open pit (A Coruña, NW Spain). Mineral Mag 72(1):399–403. https://doi.org/10.1180/minmag.2008.072.1.399

Delgado J, Juncosa R, Vázquez A, Padilla F, Vellando P, Hernández H, Fernández S (2008b) Water quality assessment in the restoration of the Meirama open pit mine, NW Spain. Part I. Hydrochemistry. In: Proceedings of 1st WSEAS international conference on environment and geological science and engineering, vol 9, pp 58–63. ISBN: 978-960-474-001-7

Delgado J, Juncosa R, Vázquez A, Fernández S, Arias M, González R, Fernández A (2010) Hydrochemical evolution of the Meirama pit lake (NW Spain) after two years of flooding. In: Proceedings of 13th international symposium on wáter-rock interaction. Taylor and Francis Group, London, pp 515–518

Delgado J, Juncosa R, Hernández H, Falcón I, Vázquez A (2011) Comparative hydrochemistry of five nested catchments located in the upper part of the Barces River watershed (A Coruña, NW Spain). Appl Geochem 26:179–182. https://doi.org/10.1016/j.apgeochem.2011.03.097

Delgado J, Juncosa R, Falcón I, Canal J (2013) Four years of continuous monitoring of the Meirama end-pit lake and its impacts in the definition of future uses. Environ Sci Pollut R 20(11):7520–7533. https://doi.org/10.1007/s11356-013-1618-9

Delgado J, Juncosa R, Jardón A, González R, Fernández A (2014) Integrating pit lakes in water basin planning: the Meirama Brown-Coal. In: Jarvie-Eggart, M (Ed), Responsible mining. Case studies in managing social and environmental risks in the developed world (Soc for Mining, Metallurgy and Exploration), Littleton, CO, pp 489–517

Denimal S, Bertrand C, Mudry J, Paquette Y, Hochart M, Steinmann M (2005) Evolution of the aqueous geochemistry of mine pit lakes-Blanzy-Montceau-les-Mines coal basin (massif Central, France): origin of sulfate contents; effects of stratification on water quality. Appl Geochem 20:825–839. https://doi.org/10.1016/j.apgeochem.2004.11.015

EC (2008) Directive 2008/105/EC of the European parliament and the council of 16 Dec 2008 on environmental quality standards in the field of water policy, amending and subsequently repealing Council directives 82/176/EEC, 83/513/EEC, 84/156/EEC, 84/491/EEC, 86/280/EEC and amending Directive 2000/60/EC. Off J Eur Commun L348: 84–97. http://eurlex.europa.eu/LexUriServ/LexUriServ.do?uri=OJ:L:2008:348:0084:0097:EN:PDF

EC (2009) Reference document on best available techniques for management of tailings and waste-rock in mining activities, January. http://eippcb.jrc.ec.europa.eu/reference/BREF/mmr_adopted_0109.pdf. Accessed 20 May 2019

EPLWG (2004) Guidelines for lake development at coal mine operations in mountain foothills of the northern east slopes. End-pit lake Working Group 2004, Report #ESD/LM/00-1. Alberta Environment, Environmental Service, Alberta, Canada

García-Rádade H, Vellando P, Padilla F, Juncosa R (2014) A coupled FE model for the joint resolution of the shallow water and the groundwater flow equations. Int J Numer Method H 24(7):1553–1569. https://doi.org/10.1108/HFF-05-2012-0123

Hernández H, Padilla F, Juncosa R, Vellando P, Fernández A (2012) A numerical solution to integrated water flows: application to the flooding of an open pit mine at the Barcés River catchment—La Coruña, Spain. J Hydrol 472–473:328–339. https://doi.org/10.1016/j.jhydrol.2012.09.040

Hirji R, Davis R (2009) Environmental flows in water resources policies, plans, and projects—case studies. Environment Dept Paper 117, The International Bank for Reconstruction and Development (World Bank). http://siteresources.worldbank.org/INTWAT/Resources/Env_Flows_Water_v2.pdf. Accessed 20 May 2019

Juncosa R, Delgado J, Padill F, Vellando P, Hernández H (2016) Improvements in Mero River Basin water supply regulation through integration of a mining pit lake as a water supply source. Mine Water Environ 35(3):389–397. https://doi.org/10.1007/s10230-015-0378-9

Juncosa R, Delgado J, Cereijo JL, Garcia D, Muñoz A (2018) Comparative hydrochemical analysis of the formation of the mining lakes of As Pontes an Meirama (Spain). Environ Monit Assess 190:526. https://doi.org/10.1007/s10661-018-6880-3

Padilla F, Hernández H, Juncosa R, Vellando P (2015) A numerical solution for the integrated analysis of water resources management: application to the Mero River watershed, La Coruña Spain. J Water Res Protect 7(10):815–829. https://doi.org/10.4236/jwarp.2015.710066

Schultze M, Pokrandt KH, Hille W (2010) Pit lakes of the central German lignite mining district: creation, morphometry and water quality aspects. Limnologica 40(2):148–155

Werner F, Bilek F, Luckner L (2001a) Implications of predicted hydrologic changes on Lake Senftenberg as calculated using water and reactive mass budgets. Miner Water Environ 20:129–139. https://doi.org/10.1007/s10230-001-8094-z

Werner F, Bilek F, Luckner L (2001b) Impact of regional groundwater flow on the water quality of an old post-mining lake. Ecolog Eng 17:133–142. https://doi.org/10.1016/S0925-8574(01)00061-1

Younger PL, Wolkersdorfer C (2004) Mining impacts on the fresh water environment: technical and managerial guidelines for catchment scale management. Mine Water Environ 23(suppl 1):2–80